Electronic Supplementary Material (ESI) for Journal of Materials Chemistry B.

Supplementary Information for Biomolecular Detection, Tracking, and Manipulation using a Magnetic Nanoparticle-Quantum Dot Platform

Kalpesh D. Mahajan[1,†], Gang Ruan[1,2,†], Greg Vieira[3,4], Thomas Porter[1], Jeffrey J. Chalmers[1], R. Sooryakumar[3], Jessica O. Winter*[1,5]

[1]*William G. Lowrie Department of Chemical and Biomolecular Engineering, The Ohio State University, Columbus, OH, USA.*
[2]*Department of Biomedical Engineering, College of Engineering and Applied Sciences, Nanjing University, China.*
[3]*Department of Physics, The Ohio State University, Columbus, OH, USA.*
[4]*Department of Physics, Rhodes College, Memphis, TN, USA.*
[5]*Department of Biomedical Engineering, The Ohio State University, Columbus, USA.*
†These authors contributed equally to this work.
*Correspondence to: winter.63@osu.edu

Supplementary Videos

Supplementary Video 1: Nanoassembly transport around a microdisc. Control is demonstrated by magnetic trapping of the nanoassembly. A reverse motion around the disk is shown from 11-16 seconds, and then the particle continues its clockwise trajectory. After 33 seconds the nanoassembly is released from the microdisc.

Supplementary Video 2: Nanoassembly transport on nanowires via vertex-to-vertex hopping.

Supplementary Video 3: Simultaneous magnetic transport of red protein (avidin) and green DNA (p53 ssDNA) nanoassemblies via vertex to vertex hopping on magnetic nanowire arrays.

Supplementary Video 4: Red, magnetic protein nanoassemblies (i.e., avidin as the molecular target, containing SPIONs) are trapped and transported from vertex-to-vertex, whereas green, non-magnetic DNA nanoassemblies (p53 ssDNA as the molecular target, containing no SPIONs) are not trapped and display motion resulting from Brownian motion or liquid flow.

Supplementary Video 5: Following addition of DNA-targeting SPION micelles, green, magnetic DNA nanoassemblies (p53 ssDNA as the molecular target, containing QDs and SPIONs) are transported, showing rapid conjugation of SPIONs to green micelle structures.

Supplementary Figures

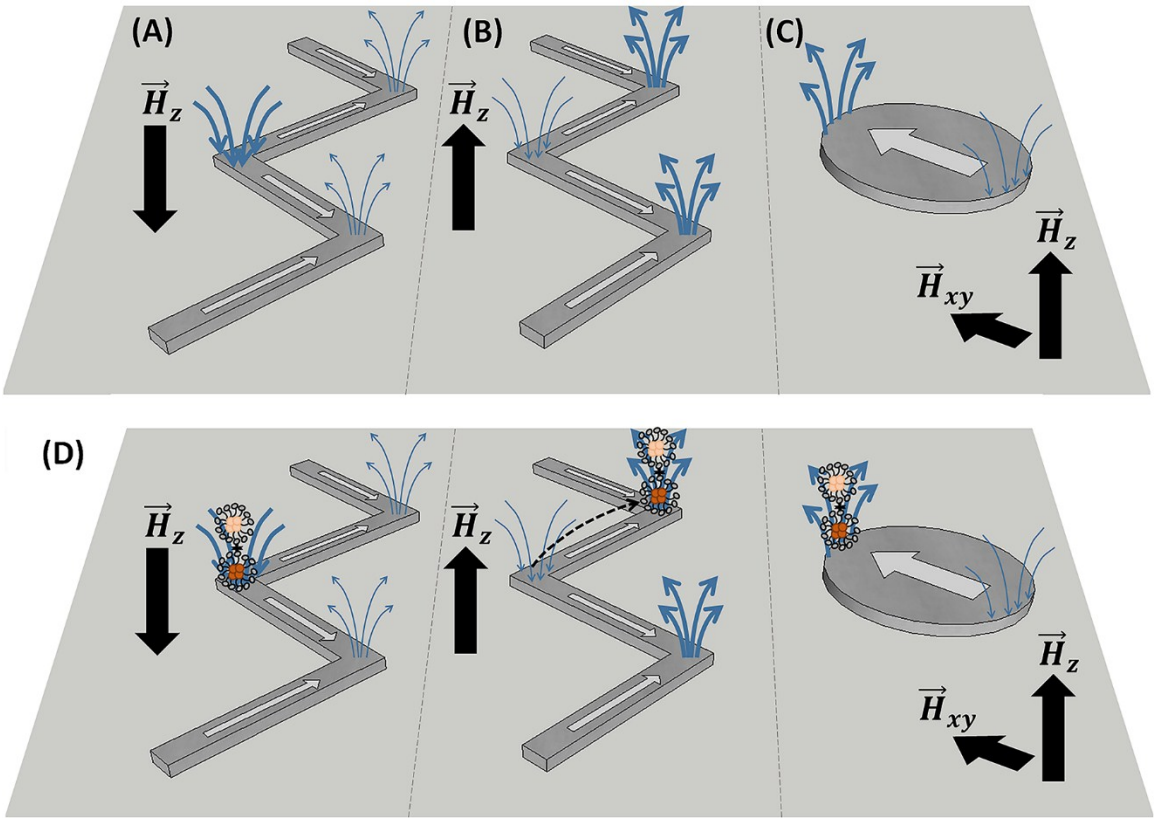

Supplementary Figure 1: Illustration of magnetic zigzag wire and disk patterns used in trapping experiments. For zigzag wires (A) and (B), magnetic domains form along wire segments (light gray arrows), resulting in locations of strong magnetic fields at wire vertices (blue arrows). These localized fields (and resulting field gradients) act as traps for magnetic nanoparticles. Upon applying a field $\vec{H}_z$ perpendicular to the platform (indicated by black block arrows), the trap strength can be tuned. Relative trapping forces are indicated by the thickness of the blue arrows at wire vertices. (C) An in-plane applied field ($\vec{H}_{xy}$) creates a magnetic domain in a disk and trapping locations at opposite edges of the disk. This domain can be rotated by rotating $\vec{H}_{xy}$. In the presence of an out-of-plane applied field $\vec{H}_z$, the trap strengths can be tuned, as with the zigzag wires. (D) Schematic illustrating trapping and transport of micelle aggregates.

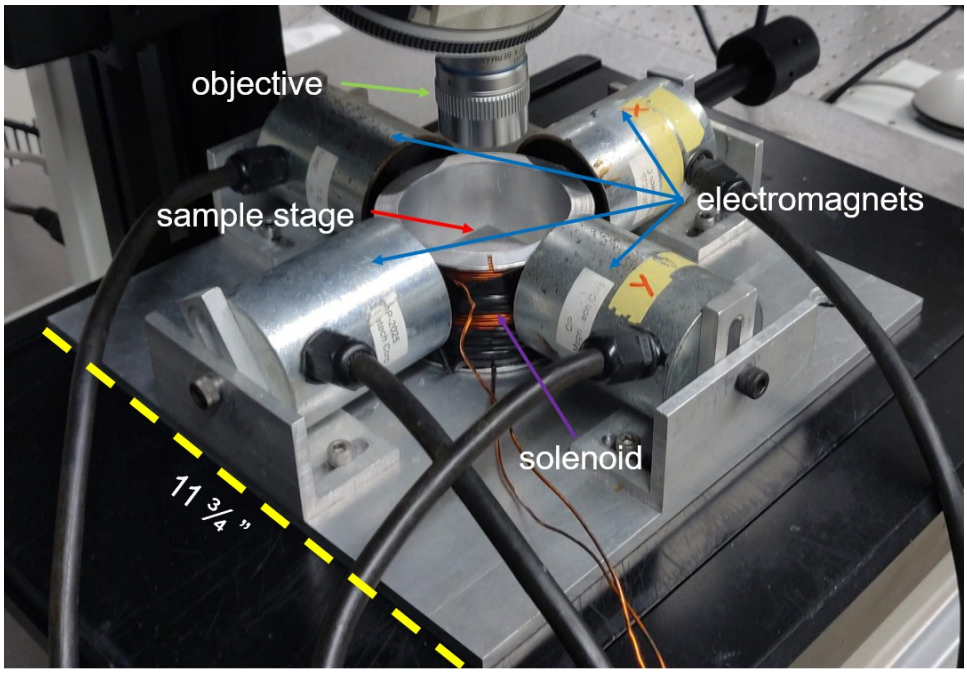

Supplementary Figure 2: Typical electromagnet setup used for these experiments. Electromagnets produce in-plane magnetic field $\vec{H}_{xy}$ whereas the solenoid coil produces the out-of-plane field $\vec{H}_z$. These fields are tunable by adjusting the current (and current direction) through the electromagnets or solenoid.

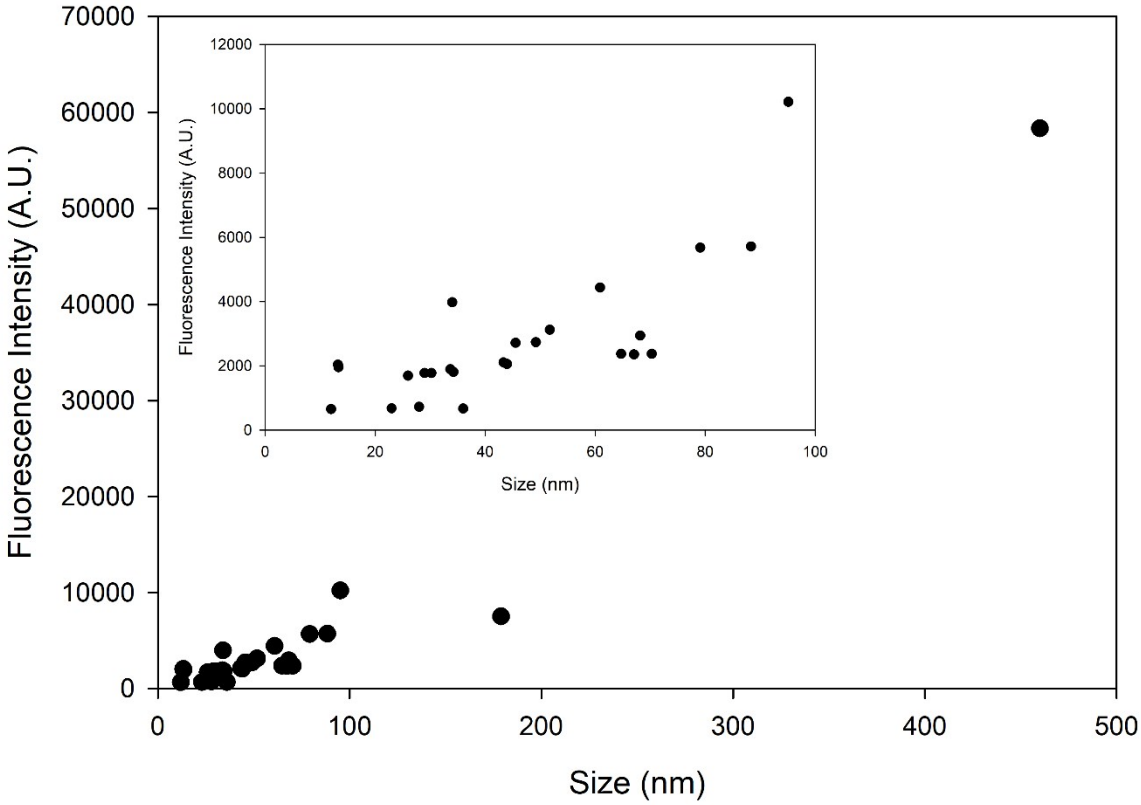

Supplementary Figure 3: Single particle tracking (SPT) analysis of micelle "nanobrick" aggregate size (diameter) vs. total fluorescent intensity as measured by fluorescence microscopy. A positive correlation between fluorescent intensity and QD-micelle cluster diameter was evidenced. Because aggregate fluorescence intensity depends on the number of micelles in the aggregate, a volumetric, or r^3, correlation between intensity and size would be expected. Also, particle sizes were clustered in the 10-100 nm range (inset), with few large aggregates formed. [Note, the fluorescence intensity here does not correspond with that of Figure 3, as different gains were used to capture larger aggregates. Fluorescence intensity is therefore reported in arbitrary units. For each experiment, QD micelles in the absence of analyte were first observed to obtain a baseline signal and aggregates were measured with reference to this baseline.]